Journal of Power Sources, 26 (1989) 93 - 102

ALLOY/CONDUCTING-POLYMER COMPOSITE ELECTRODES: ELECTROLYTES, CATHODES, AND MORPHOLOGY

M. MAXFIELD*, T. R. JOW, M. G. SEWCHOK and L. W. SHACKLETTE

Allied-Signal, Inc., P.O. Box 1021R, Morristown, NJ 07960 (U.S.A.)

Summary

Composites comprising alkali metal alloys and alkali metal doped conductive polymers constitute a class of electrode materials useful in rechargeable cells. Composite electrodes made with poly(*p*-phenylene) (PPP) and polyacetylene (PA) exhibit high rechargeability for donor doping (cation insertion) in ether electrolytes such as $NaPF_6$ in 1,2-dimethoxyethane (DME) and $LiPF_6$ in 2-methyltetrahydrofuran (MTHF), plus rechargeability, at restricted potentials, in solvents such as sulfolane and benzonitrile. Na–Pb, Li–Pb, and Li–Al alloys, formed as composites with PPP and PA, have been cycled exhaustively with excellent charge capacity retention. These composites form rechargeable cells with a variety of cation-inserting cathodes. In particular, balanced cells having Na–Pb/PPP anodes and $NaCoO_2$ cathodes have been cycled 250 times with little capacity loss. The good performance of these composites is due, in part, to the basic fibrillar morphology of the polymer, which becomes evident during cycling. After several cycles, the composites possess the fibrillar structure of pure polymer electrodes, with crystalline alloy uniformly distributed on or in the fibrils in particles of less than 0.2 μm. This structure, particularly when the fibrils are swollen with electrolyte, facilitates rapid transport of ions and electronic charge throughout the electrode.

Introduction

Composites of alkali metal alloys and conductive polymers constitute a class of electrode materials that is useful in a broad range of alkali metal based rechargeable cells. We have found that composite electrodes, each consisting of an alkali metal alloy and an alkali metal doped conducting polymer, can be formed having the best features of each constituent [1 - 4]. Our work has focused on alloy/conductive-polymer composites that perform as alloy anodes with regard to electrochemical potential and charge capacity. In room temperature cycling studies, composites such as $Na_{3.75}Pb$/poly(*p*-phenylene) (PPP) [1], LiAl/polyacetylene (PA), and $Li_{4.3}Pb$/PPP [2] have

*Author to whom correspondence should be addressed.

0378-7753/89/$3.50

exhibited cathodic potentials and high charge capacities that are comparable with values reported for alloy electrodes, plus cycle life values that are comparable with, or greater than, those of pure polymer electrodes.

We have investigated composites consisting of fine particles of alkali metal alloys of lead or aluminum dispersed in a poly(*p*-phenylene) (PPP) or polyacetylene (PA) matrix. When donor doped, these polymers are (a) electrically conductive, (b) ionically conductive, (c) electroactive, (d) self-adherent and adherent to alloys, and (e) partially elastic. The alloy component in these composites typically serves as the principal electroactive material. The polymer component maintains the activity and integrity of the electrode, regardless of alloy fragmentation incurred by the alloying and dealloying processes [2, 4], serving as current collector, metal-ion shuttle, and mechanical support. The roles of alloy and polymer are similar to those of the active and mixed-conductor phases in polyphase alloy electrodes developed by Huggins *et al.* [5]. We have found that composites are useful (a) in a variety of aprotic electrolytes, (b) in cells with a variety of cation-inserting cathode materials, and (c) in applications requiring high charge capacity for several hundred cycles. In this paper we discuss these electrodes in relation to their use with different electrolytes and with different cathodes. We will also consider the role which their morphology plays in determining their performance as electrode materials.

Electrolytes

Reductively stable aprotic solutions and fused salts have been shown to be suitable for use with composite anodes. By far, the most important of these are liquid ether electrolytes containing alkali metal salts of hexafluorophosphate and alkyl borate anions selected, principally, for their stability toward reduced conductive polymers (Table 1). Tetrahydrofuran (THF), 1,2-dimethoxyethane (DME), and 2-methyltetrahydrofuran (2-MTHF) solutions of $NaPF_6$ and $LiPF_6$ have been used most extensively due to their reductive stability combined with oxidative stability and good ionic conductivity. Ether solutions of tetraphenylborate salts exhibit

TABLE 1

Stability windows and a.c. conductivities for electrolytes

Electrolyte salt	Solvent	Stability range (V *vs.* Li/Li^+)	Conductivity (mS cm^{-1})
1.5 M $NaPF_6$	DME	< 0.25 - 3.9	10.6
1.5 M $LiPF_6$	2-MTHF	< 0.1 - 3.4	2.5
0.2 M $LiB(C_6H_5)_4$	THF	< 0.1 - 3.0	1.2
1.0 M $LiPF_6$	THF	0.1 - 3.3	11.7
1.5 M $LiPF_6$	MTFE	0.1 - 3.8	5.8

excellent reductive stability but limited oxidative stability and conductivity. The PF_6-containing electrolytes have been used in whole cells, having high potential cathodes, that demonstrate high coulombic efficiencies in repeated deep cycles. MPF_6 solutions of methyltetrahydrofurfuryl ether (MTFE) also appears to have an attractive stability window and good ionic conductivity.

In some cases mixed solvents produce electrolytes having enhanced conductivities. For example, 1.5 M $LiPF_6$ in a 5:1 mixture of 2-MTHF and MTFE has a room temperature conductivity of 6.2 mS cm^{-1}.

Other electrolytes, exhibiting limited stability to reduced conductive polymers, are of interest due to their high oxidative stability (Table 2). Among these electrolytes are perchlorate salts and hexafluorophosphate salts dissolved in benzonitrile, and sulfolane.

TABLE 2

Electrolytes with limited potential stability

Electrolyte salt	Solvent	Stability range (V *vs.* Li/Li^+)	Conductivity (mS cm^{-1})
1.0 M $LiPF_6$	sulfolane	0.9 - 4.5	2.3
0.5 M $NaPF_6$	benzonitrile	0.9 - 4.5	2.9
1.0 M $LiClO_4$	PC	1.6 - 4.4	4.5
1.0 M $LiClO_4$	PC/BS (9:1)	1.6 - 4.4[a]	3.5

[a]Effectively 0.1 - 4.4 V when used with PA-covered anode.

In special cases, highly reduced PA electrodes can be used in electrolytes which are otherwise incompatible with composite anode components. For example, cyclic sulfonate esters, 1,3-propane sultone (PS) and 1,4-butane sultone (BS), are reactive at potentials below 0.9 V *versus* Li/Li^+, but the reaction with reduced polyacetylene (PA) forms an ionically conductive barrier film enabling the underlying conductive polymer–alloy composites to cycle reversibly in these oxidatively stable electrolytes [6]. A protective film on PA is also formed when the polymer is reduced in $LiClO_4$ in propylene carbonate (PC) containing small amounts of PS or BS. LiAl/PA electrodes can be cycled with excellent efficiency in $LiClO_4$ dissolved in propylene carbonate (PC):BS (50:1 by volume). Thus, PC:BS has an effective stability window of 0.1 - 4.1 V when used with PA-covered anodes. Similar protective films are formed on PA electrodes when ethylene oxide and propylene oxide are added to $LiClO_4$ in PC.

Balanced whole cells

We have conducted extensive testing of cells using Na_yPb/PPP anodes, and limited testing on a selection of cells using anodes comprising either Li_yPb or LiAl with either PPP or PA.

TABLE 3

Rechargeable cells with alloy–polymer composite anodes

Cathode	Demonstrated range of x	Anode	Average discharge voltage
Na_xCoO_2	0.5 - 1.0	Na_yPb/PPP	2.5
$Li_xVO_{2.17}$	0 - 0.6	Li_yPb(Al)/PPP(PA)	2.0
$Li_xVO_{2.5}$	0 - 0.4	Li_yPb(Al)/PPP(PA)	2.0
Li_xMnO_2	0 - 0.5	Li_yPb(Al)/PPP(PA)	2.4
Li_xCoO_2	0.5 - 1.0	Li_yPb/PA[a]	3.6

[a]PA is surface treated with butane sultone to prevent reaction with propylene carbonate electrolyte.

Nearly balanced, flooded test cells have been assembled from composite anodes coupled with cathodes formed of Na_xCoO_2, $Li_xVO_{2.17}$ (*i.e.*, V_6O_{13}), $Li_xVO_{2.5}$ (V_2O_5), Li_xMnO_2, and Li_xCoO_2 (Table 3). Cells of each type have been cycled continuously at 0.5 - 1.0 mA cm^{-2}. A sodium-based cell was cycled 250 times between 3.1 and 1.8 V with 16% capacity loss [7]. An $Li_xVO_{2.17}$ cell was cycled 28 times between 2.7 and 1.4 V with a 10% capacity loss. An $Li_xVO_{2.5}$ cell was cycled 10 times between 2.9 and 2.0 V with essentially no capacity loss. An Li_xMnO_2 cell was cycled 35 times between 3.2 and 2.0 V with a 20% capacity loss. Finally, a cell consisting of an LiAl/PA anode and an $LiCoO_2$ cathode in $LiClO_4$ in PC (2.5% BS) was cycled 10 times between 4.0 and 2.6 V with a 22% capacity loss. In most cases, the capacity loss was attributable to degradation of the cathode.

Typical anodes were fabricated with 80% by weight alloy (*e.g.*, $Na_{3.75}Pb$, $Li_{4.3}Pb$, $Li_{1.3}Al$), 18% conductive polymer (*e.g.*, Na–PPP, Li–PPP, Li–PA), and 2% binder (EPDM rubber). Typical cathodes were fabricated with 80% active material, 16% carbon black, and 4% binder (EPDM rubber or Teflon). Procedures described in the literature were followed to prepare $Na_{0.67}CoO_2$ (P2 phase) [8], $VO_{2.17}$ [9], and MnO_2 [10]; $VO_{2.5}$ and $LiCoO_2$ were used as received (Cerac).

Packaged cells

We have conducted preliminary tests on sealed, fully packaged AF-sized cells of $Na_{3.75}Pb$/PPP *versus* $Na_{0.6}CoO_2$ and $Li_{4.3}Pb$/PPP *versus* $VO_{2.17}$. Sodium AF cells have demonstrated 1.7 W h (160 W h l^{-1}). Lithium AF cells have demonstrated 1.8 W h (170 W h l^{-1}).

Cycling performance of composite anodes in half cells

Cycling performance, which was representative of composite electrodes, was obtained by cycling test composite electrodes *versus* excess cathodes

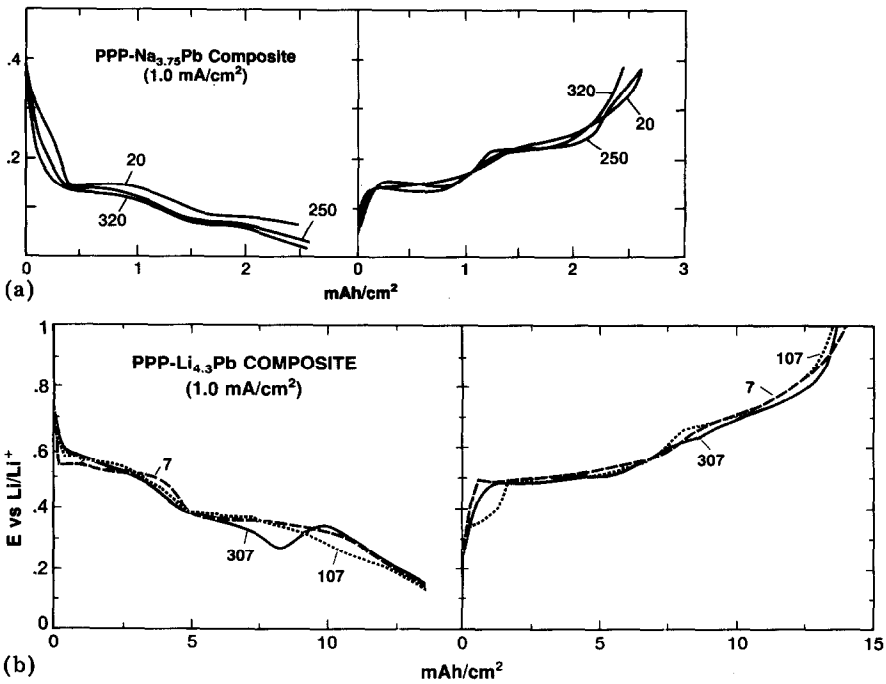

Fig. 1. Potential plotted *vs.* capacity (mA h cm^{-2}) of composite anodes cycled at 1 mA cm^{-2} at 18 °C in anode-limited cells: (a) $Na_{3.75}Pb$/PPP (50%/43% by weight) *vs.* an Na/Na^+ reference electrode; (b) $Li_{4.3}Pb$/PPP (80%/18% by weight) *vs.* an Li/Li^+ reference electrode.

or *versus* another composite electrode. In such anode-limited cells, composite anodes have demonstrated excellent performance during exhaustive deep cycling. In particular, composites of PPP with either Na_yPb or Li_yPb have demonstrated over 320 cycles, where about 70% of theoretical capacity was utilized on each cycle, with less than 5% loss in electroactivity and without appreciable buildup of resistance (Fig. 1). An Li_yPb/PPP composite was discharged (oxidized) twice in succession, after standing fully charged for 40 days, with 98% coulombic efficiency each time (Fig. 2).

Table 4 presents a comparison of the capacity of various composite anodes. The gravimetric capacities listed in Table 4 were calculated based on the masses of binder, conducting polymer, and alloy. The mass of alloy was based on the compositions, $Li_{1.3}Al$, $Li_{4.3}Pb$, and $Na_{3.75}Pb$. The volumetric capacities were calculated from the dimensions of the initial dry and porous composite films. Some swelling of the polymer components by electrolytes, which is essential to performance of the composites, decreases the effective volumetric capacities by a small amount. However, comparable capacities were demonstrated by composite anodes which were tightly confined in sealed AF cells.

The observed decline of capacity with cycling can be empirically modelled by an equation,

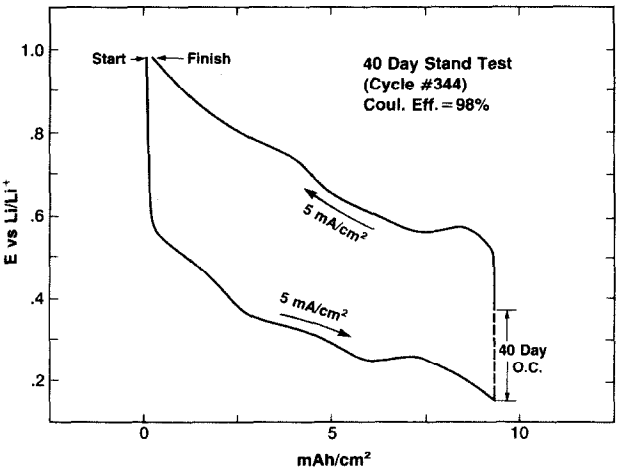

Fig. 2. Potential plotted *vs.* capacity (mA h cm^{-2}) of an $Li_{4.3}Pb$/PPP (80%/18% by weight) film during a 5 mA cm^{-2} cycle that was interrupted for 40 days between reduction (charge) and re-oxidation (discharge).

TABLE 4

Performance of alloy–polymer composite anodes

Composition (wt.%)	Initial gravimetric capacity (mA h g^{-1})	Initial volumetric capacity (mA h cm^{-3})	Number of cycles to 80%
$Na_{3.75}Pb$:PPP (50:43)	200	400	1000
$Na_{3.75}Pb$:PPP (79:19)	234	450	500
$Li_{4.3}Pb$:PPP (80:18)	230	450	1000
$Li_{4.3}Pb$:PA (24:69)	280	370	100
LiAl:PA (11:89)	220	130	80

PA = polyacetylene.
PPP = poly(*p*-phenylene).
Balance of composition is binder (poly(propylene) EPDM rubber).

$$Q_n = Q_i(f)^{n-n_i} \quad (1)$$

where Q_n is the discharge capacity of the nth cycle and Q_i is the discharge capacity of an arbitrary previous cycle, n_i. The quantity f defines a loss factor of the composite. Using eqn. (1), the number of cycles having >80% initial capacity ($n_i = 1$) can be projected. These values are given in the right-

hand column of Table 4. In general, sodium–lead and lithium–lead composites with PPP exhibit capacities and cycle life values that are superior to those of composites containing either LiAl as the alloy or PA as the conductive polymer.

Morphology of Na–Pb/PPP and Li–Pb/PPP composite electrodes

PPP composites, which have performed well in half cells and balanced cells, were prepared by mechanically mixing their components and, with the aid of elastomer binder, forming the mixtures into films. Thus formed, these films consisted of particles of pure alloy bounded by regions of pure polymer. This initial morphology is consistent with observed reduction and oxidation potentials of composite electrodes, but is inconsistent with their complex impedance behavior.

We have previously examined the electrochemistry of a composite electrode by conducting voltage step cycling [11] and frequency response impedance studies of polymer films, powdered alloys formed as films, and composite films [1, 12]. According to the voltage step study, the redox processes of a composite are a combination of the separate redox processes of its polymer and alloy components. Even after exhaustive cycling, the redox processes of a composite appear to be independent and essentially unchanged.

On the other hand, the complex impedance behavior of a composite evolves with cycling. After several cycles it resembles the impedance behavior of pure polymer electrodes, particularly at low frequencies where polymer electrodes display high effective capacitance values (214 F g^{-1} for Na–PPP [1] and 350 F g^{-1} for Na–PA [12]).

Recently, we have investigated the actual morphology of PPP composites by scanning electron microscope (SEM) and an X-ray diffractometer (XRD) and obtained data which reconcile the voltage step and impedance studies.

Samples of the Na_yPb/PPP and Li_yPb/PPP film electrodes, formed as described in the section on balanced cells, were examined by SEM and XRD both before, and after, each electrode was exhaustively cycled. In the SEM, surface and cross-sectional features of greater than 40 Å were resolved, and relative distributions of polymer and alloy were mapped with 1000 Å resolution. Crystalline phases and crystallite sizes of the alloys and PPP were indicated by diffraction patterns.

According to their SEM micrographs, each composite was formed as a porous aggregate of alloy particles dispersed in PPP granules. In the Li_yPb composite, which was formed by simple mixing, the alloy particles were 2 - 20 μm in diameter. In the Na_yPb composite, which was formed by repeated mixing and pelletizing, the alloy particles were smeared out, but alloy was still localized in discreet regions 10 - 30 μm across. In both cases, microprobe mapping indicated Pb in the alloy regions and not in the PPP.

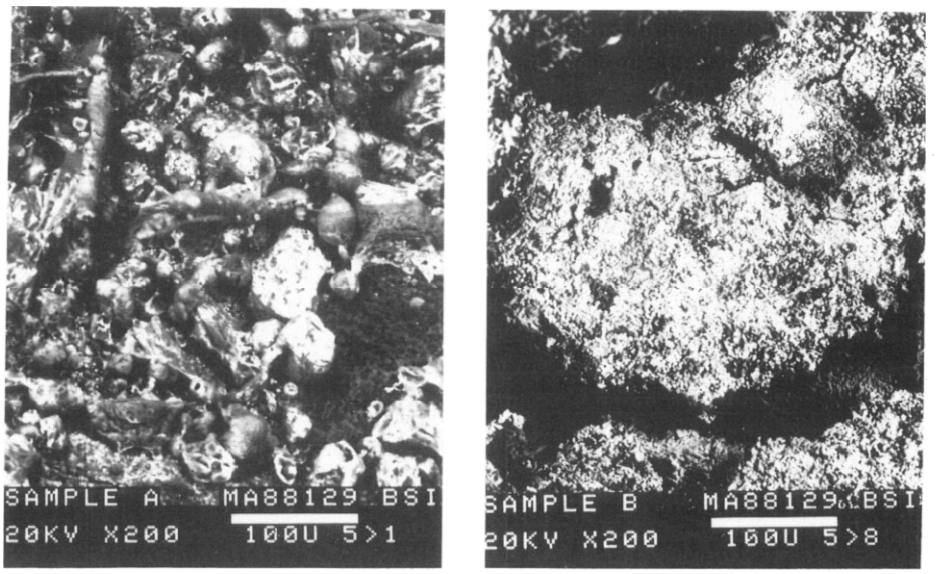

Fig. 3. Micrographs of an $Na_{3.75}Pb$/PPP composite film using backscatter electrons to distinguish lead-containing surfaces (light) from polymer surfaces (grey): (left) prior to electrochemical cycles; (right) after 250 cycles.

After 250 cycles (with less than 5% capacity loss), the Na_yPb/PPP electrode was shown in the SEM to consist of a fibrillar polymer network with a dispersion of submicron Pb-containing particles adhering to the fibrils (Fig. 3). After 350 cycles (with 5% capacity loss), the Li_yPb/PPP electrode appeared as a fibrillar polymer network having no discrete Pb-containing particles (Fig. 4). Instead, microprobe mapping showed that Pb, possibly in the form of particles smaller than 0.1 μm, was distributed within the polymer fibrils.

According to XRD analysis, alloy phases in the cycled samples were different from those in the uncycled samples, but there was remarkably little difference in crystallite size between the uncycled and cycled samples. Alloy crystallite size in the uncycled Na_yPb composite was 160 - 180 Å and 102 - 130 Å in the cycled sample. Alloy crystallite size in the uncycled Li_yPb composite was 290 - 350 Å and 230 - 390 Å in the cycled sample. The crystallite size of the PPP component of both composites remained at 45 - 55 Å before, and after, cycling.

We conclude that deep cycling of these composite electrodes engenders swelling and disaggregation of PPP fibrils in addition to continuous fragmentation and redistribution of alloy particles. Cycling causes the alloy to become uniformly distributed on, or in, polymer fibrils and to be fragmented into submicron particles. Ultimately, particles less than 2000 Å and larger than 230 - 390 Å are produced. Thus, the alloy and the polymer components remain as discrete electroactive materials throughout cycling

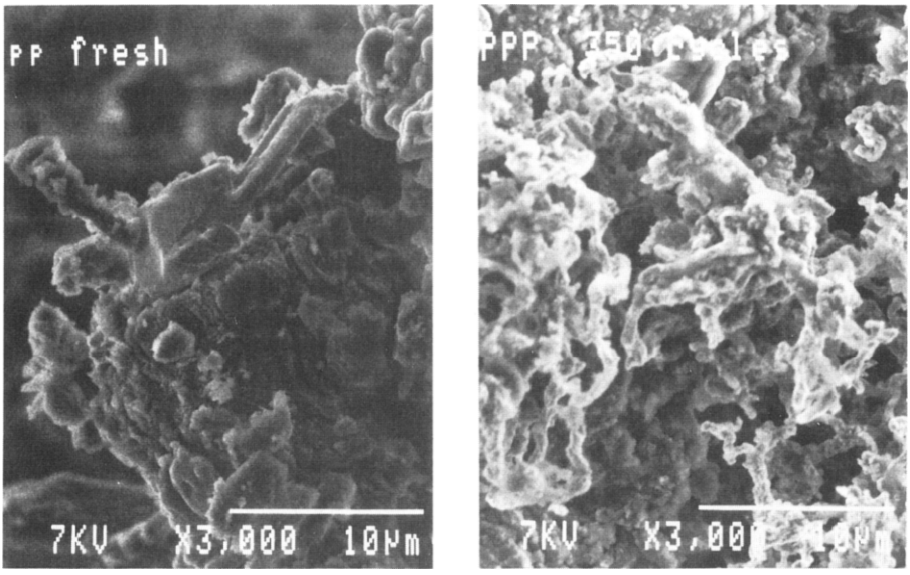

Fig. 4. Micrographs of an $Li_{4.3}Pb$/PPP composite film, using secondary electrons: (left) prior to cycling; (right) after 350 cycles.

(as suggested by the voltage *versus* composition behavior), but acquire the structural form similar to that of pure conductive polymers (as suggested by their impedance behavior).

Conclusion

We have shown that alloy/conductive-polymer composite electrodes exhibit high performance in a variety of electrochemical systems. The performance of the composites is due, in part, to the physical structure and morphology which the polymer assumes during the operation of the cells. After extensive cycling, the microstructure of the composite electrodes consists of fibrillar conductive polymer, with the alloy distributed uniformly on, or in, the fibrils in particles of less than 2000 Å. Thus, the complex impedance behavior of composite electrodes, which is sensitive to morphology, reflects the kinetic behavior of conducting polymer electrodes. Alloy and polymer crystallites remain intact throughout cycling. Thus, the composite continues to be dominated by the redox behavior of the alloy in that a level voltage is maintained and a high capacity is achieved.

The structure of the composite facilitates rapid ion transport through the electrode by minimizing the necessity for extensive solid-state diffusion in the alloy alone. It also maximizes electrical and mechanical contact between alloy and polymer, thereby preserving the rate capability and the electrochemical capacity of the composite with cycling.

References

1 T. R. Jow, L. W. Shacklette, M. Maxfield and D. Vernick, *J. Electrochem. Soc., 134* (1987) 1730.
2 M. Maxfield, T. R. Jow, S. Gould, M. G. Sewchok and L. W. Shacklette, *J. Electrochem. Soc., 135* (1988) 299.
3 L. W. Shacklette, M. Maxfield, S. Gould, J. F. Wolf, T. R. Jow and R. H. Baughman, *Synth. Met., 18* (1987) 611.
4 J. O. Besenhard, P. Komenda, A. Paxinos and E. Wudy, *Solid State Ionics, 18 & 19* (1986) 823.
5 R. A. Huggins, *J. Power Sources, 22* (1988) 341.
6 M. Maxfield, J. F. Wolf, G. G. Miller, J. E. Frommer and L. W. Shacklette, *J. Electrochem. Soc., 133* (1986) 117.
7 T. R. Jow and L. W. Shacklette, *J. Electrochem. Soc., 136* (1989) 1.
8 L. W. Shacklette, T. R. Jow and L. B. Townsend, *J. Electrochem. Soc., 135* (1988) 2669.
9 K. West, B. Zachau-Christiansen, M. J. L. Ostergard and T. Jacobsen, *J. Power Sources, 20* (1987) 165.
10 J. Attenburrow, A. F. B. Cameron, J. H. Chapman, R. M. Evans, B. A. Hems, A. B. A. Jansen and T. Walker, *J. Chem. Soc.,* (1952) 1094.
11 L. W. Shacklette, J. E. Toth, N. S. Murthy and R. H. Baughman, *J. Electrochem. Soc., 132* (1985) 1529
12 T. R. Jow and L. W. Shacklette, *J. Electrochem. Soc., 135* (1988) 541.